Available online at www.sciencedirect.com
SCIENCE DIRECT
Ocean Engineering 33 (2006) 788–797
OCEAN ENGINEERING
www.elsevier.com/locate/oceaneng

Technical note

# Risk analysis for capsizing of small vessels

K. Al-Salem*, W. Al-Nassar, A. Tayfun

*Kuwait institute for scientific research, Department of Coastal & Air Pollution, 13109 Safat, Kuwait*

Received 27 December 2004; accepted 28 July 2005
Available online 10 October 2005

**Abstract**

Vessel accidents during stormy weather conditions over Kuwait's coastal waters are one of the major concerns for insurance and re-insurance companies, since such accidents can result in not only material losses but also losses of lives. In order to determine insurance rates for different types of vessels and their operators, it is desirable to estimate the risk or probability of occurrence of an accident and the resulting expected damage or losses associated with a given vessel type under the local wave conditions first. Therefore, there is a national need for such a study to provide this type of basic information on the risks or probabilities of vessel accidents caused by high waves within the Kuwait's territorial waters. The main objective of this study is thus to provide such information for the local and international agencies and companies concerned with sailing operations and maintenance, navigational safety, and particularly insurance of small recreational and commercial vessels. The study was carried out with the financial support of M/s Warba Insurance Company and the Kuwait Foundation for the Advancement of Sciences, Kuwait.


*Keywords:* Insurance; Kuwait's territorial waters; Prototype

## 1. Project description

The main objective of this study is to provide estimated measures of risk for capsizing of vessels for the local and international insurance agencies concerned with sailing operations and navigational safety, and particularly insurance of small recreational and commercial vessels. The information required includes the simulation of vessel stability under adverse wave conditions, the wind-wave climate of Kuwait's marine environment,

* Corresponding author. Tel.: +965 4836 100; fax: +965 4815 192.
*E-mail address:* ksalem@safat.kisr.edu.kw (K. Al-Salem).

0029-8018/$ - see front matter 
doi:10.1016/j.oceaneng.2005.07.003

development of a small-vessel risk map for Kuwait's territorial waters under extreme wave conditions, and tables listing capsize probability risks associated with various small vessels of varying sizes operational within Kuwait's territorial waters.

## 2. Simulation of extreme wave conditions within Kuwait's territorial waters

In order to simulate extreme wave conditions over the three coastal sectors of Kuwait as shown in Fig. 1, larger scale wind data covering the whole of the Arabian Gulf have been utilized. The data have spatial and temporal resolutions of $0.5 \times 0.5°$ and 3 h, respectively, and cover 8 years of meteorological forecasts obtained from ECMWF, UK. The data set is rather extensive, making wind-wave simulations based on the total set rather impractical. Intuitively and also guided by the nature of wind-wave generation processes, it is rational to regard certain wind directions as being more likely to generate the largest waves. These cover winds blowing from the South-to-East (SE) quadrant with potentially the largest fetch lengths along the SE axis toward Kuwait. The second quadrant where winds blow

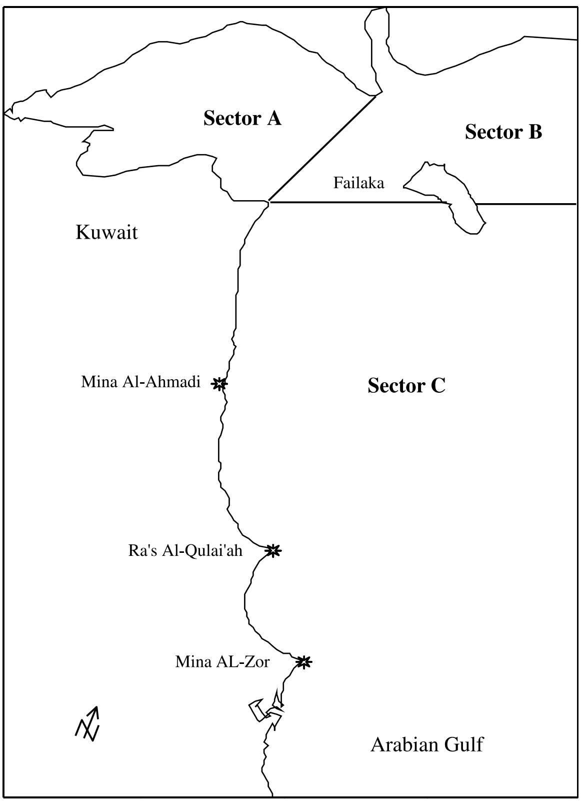


Fig. 1. Three sectors (A, B, C) utilized to define Kuwait's territorial waters. Prototype spectrum density: JONSWAP (limited fetch).

from and are likely to generate larger waves is the North-to-West (NW) quadrant. For the SE quadrant, the generation area includes all the grid points over the Arabian Gulf. In contrast, for the NW quadrant, only the grid points over the territorial waters of Kuwait need to be considered. For both cases, largest waves are likely to be generated by wind patterns with the largest energy over the respective generation zone. A simple straightforward measure of this is represented with the average (kinetic) wind energy per unit resolution grid ($0.5\times0.5^{\circ}$), given proportionally by wind speeds squared and averaged over each respective wind-wave generation area of the two quadrants. In this process, only the winds coming from the NW and SE need to be included, leading to a time series of the average wind energy measures from which the monthly maxima and their times of occurrence can be filtered out. Obviously, such maxima do not occur simultaneously for the two different quadrants, and so there would be two sets of eight maxima, or equivalently $2\times8=16$ peak energy wind patterns for each month for the 8-year data from 1993 to 2000 as in (Al-Salem, 2004). These patterns are then used in the spectral wind-wave generation numerical model to simulate the corresponding wave field properties at the three coastal sectors as shown in Fig. 1, each summarized in terms of the significant wave height $H_{\rm s}=4m_0^{1/2}$ and spectral 'mean' wave period $T$. From these, the estimates of eight significant wave heights $H_{\rm s}$ representative of the monthly extreme sea-state conditions for the 8-year period from 1993 to 2000 would readily follow as the principal input for the capsize risk analysis.

## 3. Capsize risk under storm waves

### *3.1. Capsizing wave heights*

The experiments in the laboratory were done with a 1-m long model using a length scale of $N_L=19$. Based on preliminary trials with six 1-m models with varying dimensionless length ($L$), beam ($B$), depth ($D$) and draught ($T$) ratios, capsize conditions were simulated with irregular waves generated from a JONSWAP type spectral density representative of full-scale conditions with a significant wave height $H_{\rm s}=7.14$ m and spectral modal period $T=7.34$ s, as shown in Fig. 2. This figure follows from multiplying the model wave heights by the length scale $N_L=19$ and model wave periods by the time scale $N_T=(N_L)^{1/2}\approx4.36$. Typically, capsize occurs with larger breaking waves striking the models sideways within approximately 2 h under the prototype conditions. A wave-by-wave analysis of a 5-min segment of waves recorded in the experiments is shown in Fig. 3. The approximate region indicative of wave heights ($H$) and periods ($T$) causing capsize is shown in hollow triangles. As a critical threshold wave height, the average of these given by $H_{\rm c}\approx8.08$ m (capsize wave height) can thus be used as the capsizing wave height. This simply means that a full-scale boat of about 19 m long would capsize with certainty within a period of about 2 h by the action of waves with heights greater than about $H_{\rm c}\approx8.08$ m under the simulated prototype extreme conditions. Since the length scale for this case is $N_L=19$, this threshold wave height can be scaled up or down to other prototype boat lengths within the same ensemble of the length, beam, depth and draught ratios tested in the lab. The results of this extrapolation are summarized in Fig. 4, showing the threshold

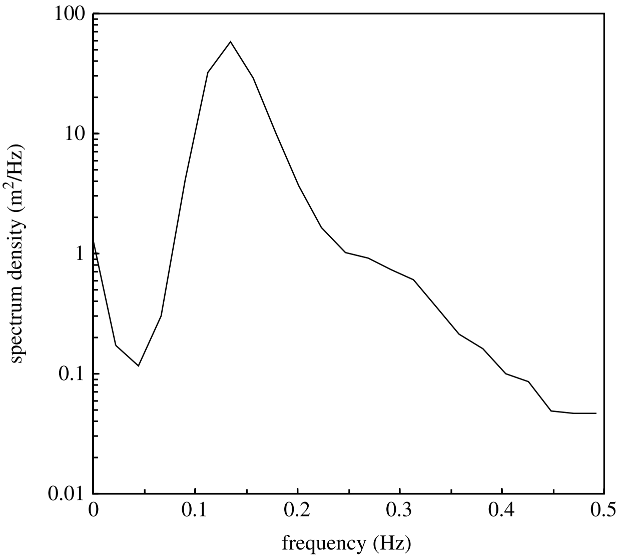


Fig. 2. Prototype extreme wave conditions simulated in lab experiments corresponding to capsize of a 19-m full scale boats. Significant wave height: 7.14 m. Peak frequency (period): 0.134 Hz (7.44 s).

capsize wave height $H_c$ as a function of boat length $L$ varying from 1 to 25 m. The range of boat lengths relevant to Kuwait is from 3 to 25 m. The figure is valid for all vessel sizes with hull forms over the range of dimensionless ratios $3.5 < L/B < 4.1$, $4.6 < B/T < 5.4$, and $2.2 < D/T < 2.8$. These represent a relatively wide range of hull shapes, and will thus be assumed to be representative of vessels in Kuwait also.

### 3.2. Modeling capsize risk levels

To describe the basic rationale and principal assumptions of the capsize risk analysis, it is first noted that the distribution of heights $H$ of wind waves, given $H_s$, is described approximately by the Rayleigh probability density:

$$p\left(\frac{H}{H_s}\right) = 4\frac{H}{H_s^2}\exp\left(-2\frac{H^2}{H_s^2}\right) \quad (H \geq 0) \tag{1}$$

Thus, given $H_s$, the probability that $H$ exceeds a specified level, say $H^*$, is given by the area under $p(H/H_s)$ over $(H^*, \infty)$, i.e.

$$E\left(\frac{H^*}{H_s}\right) = \exp\left(-2\frac{H^{*2}}{H_s^2}\right) \tag{2}$$

This probability is often referred to as the exceedance probability associated with the threshold $H^*$, given $H_s$.

Next, it is noted that wind-wave simulations provide two integral wave characteristics, $H_s$ and $T$, as opposed to an ensemble of actual wave heights and periods $\{H,T\}$. $H_s$

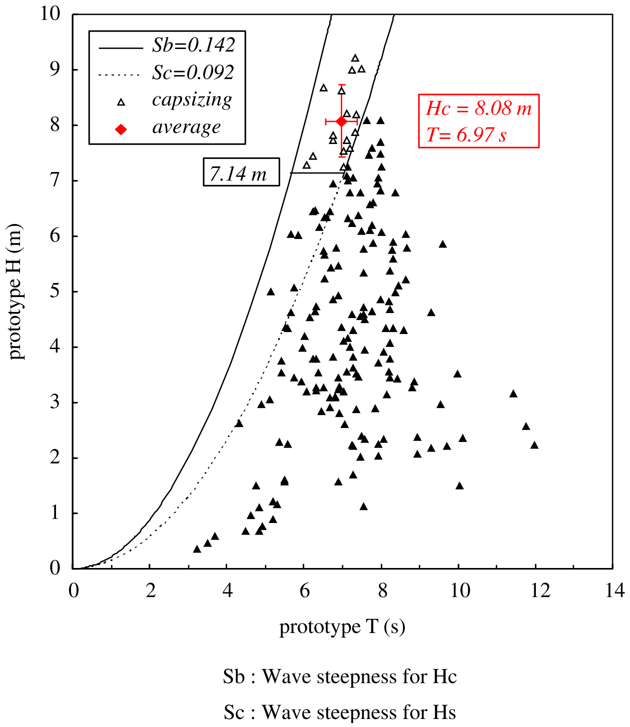


Fig. 3. Scatter diagram of wave heights and periods for prototype Extreme conditions: capsizing wave heightperiod data are shown in hollow triangles for a 19-m full scale boat and approximately fall in the region defined by H ≥ 7.14 m and S ≥ 0.092. Sb: wave steepness for Hc. Sc: Wave steepness for Hs.

represents very nearly the mean or statistical average of the largest (1/3)rd wave heights, and $T$ the corresponding period based on the spectral mean frequency. In principle, once $H_s$ is known or predicted, then it is clear that the distribution of wave heights in that sea state can be described with the Rayleigh probability distribution as in Eq. (1). There are several candidates used in coastal engineering for that distribution, including the Gumbel distribution, two-parameter Weibull distribution, and lognormal distribution given, respectively, by:

Gumbel:

$$F(H_s) = \exp[-\exp(-\alpha(H_s - \beta)] \tag{3}$$

Weibull:

$$F(H_s) = 1 - \exp\left[-\left(\frac{H_s}{\beta}\right)^{\alpha}\right] \tag{4}$$

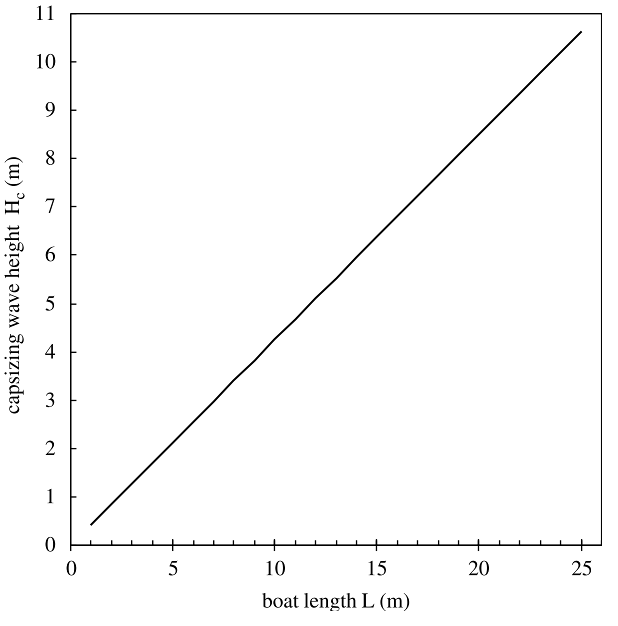


Fig. 4. Threshold capsizing wave heights $H_c$ associated with varying boat length $L$.

Lognormal:

$$F(H_s) = \frac{1}{\sqrt{2\pi}\sigma}\int_0^{H_s}\frac{1}{H_s}\exp\left[-\frac{1}{2}\left(\frac{\ln H_s - \mu}{\sigma}\right)^2\right]\mathrm{d}H_s = Q\left(\frac{\ln H_s - \mu}{\sigma}\right) \tag{5}$$

where

$$Q(x) = \frac{1}{\sqrt{2\pi}}\int_{-\infty}^{x}\exp\left(-\frac{u^2}{2}\right)\mathrm{d}u \tag{6}$$

The preceding can easily be transformed to the following forms:

Gumbel:

$$Y = \ln(-\ln(F)) = -\alpha H_s + \alpha\beta \tag{7}$$

Weibull:

Table 1
Constants for unbiased plotting position

| Distribution | $c_1$ | $c_2$ |
|---|---|---|
| Log-normal | 0.25 | 0.125 |
| Gumbel | 0.44 | 0.12 |
| Weibull | $0.20+0.27/\alpha$ | $0.20+0.23/\alpha$ |

$$Y = \ln(-\ln(E)) = \alpha \ln H_s - \alpha \ln \beta, \quad E = 1 - F \tag{8}$$

Lognormal:

$$Q^{-1}(F) = \frac{1}{\sigma} \ln H_s - \frac{\mu}{\sigma} \tag{9}$$

These transformations indicate that the left sides of all three expressions are a linear function of either $H_s$ or $\ln H_s$. Thus, given $N$ values of annual max $H_s$, we simply try to determine the two parameters involved in any one of the three extremal distributions via the least-squares technique and choose that one with the largest coefficient of multiple determination $R^2$. Given $N$ ranked values of max $H_s$, the corresponding estimates for $F$ and $E$ are given by the plotting position formulas:

$$F = 1 - \frac{i - c_1}{N + c_2} \tag{10}$$

$$E = \frac{i - c_1}{N + c_2} \tag{11}$$

where it is understood that $i = 1, 2, \ldots, N$. In the simplest estimates of $F$ and $E$, $c_1$ and $c_2$ are two coefficients that normally assume the values 0 and 1, respectively. These tend to lead to somewhat biased estimates. Other values are known, as shown in Table 1 below, to obtain so-called unbiased plotting position for each distribution.

Once an appropriate distribution for the annual max $H_s$ is determined, then the total capsize risk or probability follows by numerical integration from the conditional risk $E(H^*/H_s) = E(H_c/H_s)$ in the form:

$$R = \int_0^\infty E\left(\frac{H_c}{H_s}\right) \mathrm{d}F(H_s) \tag{12}$$

In the present case, comparisons indicated that the lognormal distribution does slightly better than the Gumbel and Weibull distributions, though the sample size $N = 8$ is

Table 2
Parameters for the extremal log-normal distribution fitted to monthly wave heights, 1993–2000

| Month | Sector A | | | Sector B | | | Sector C | | |
|---|---|---|---|---|---|---|---|---|---|
| | $\mu$ | $\sigma$ | $R^2$ | $\mu$ | $\sigma$ | $R^2$ | $\mu$ | $\sigma$ | $R^2$ |
| January | −0.664 | 0.420 | 0.902 | −0.605 | 0.365 | 0.813 | 0.066 | 0.335 | 0.914 |
| February | −0.634 | 0.375 | 0.8853 | −0.516 | 0.311 | 0.9524 | 0.072 | 0.437 | 0.822 |
| March | −0.411 | 0.355 | 0.969 | −0.316 | 0.387 | 0.741 | 0.298 | 0.328 | 0.977 |
| April | −0.645 | 0.298 | 0.908 | −0.557 | 0.274 | 0.946 | 0.008 | 0.271 | 0.843 |
| May | −0.673 | 0.326 | 0.896 | −0.584 | 0.351 | 0.862 | 0.032 | 0.250 | 0.895 |
| June | −0.732 | 0.417 | 0.721 | −0.611 | 0.396 | 0.838 | 0.029 | 0.466 | 0.782 |
| July | −0.688 | 0.467 | 0.771 | −0.688 | 0.467 | 0.771 | 0.095 | 0.517 | 0.989 |
| August | −0.734 | 0.394 | 0.929 | −0.694 | 0.337 | 0.798 | −0.084 | 0.557 | 0.868 |
| September | −0.896 | 0.226 | 0.772 | −0.860 | 0.169 | 0.576 | −0.214 | 0.234 | 0.915 |
| October | −0.938 | 0.306 | 0.764 | −0.902 | 0.290 | 0.640 | −0.217 | 0.325 | 0.869 |
| November | −0.653 | 0.348 | 0.913 | −0.558 | 0.315 | 0.913 | 0.119 | 0.352 | 0.879 |
| December | −0.790 | 0.286 | 0.852 | −0.681 | 0.224 | 0.865 | 0.000 | 0.220 | 0.878 |

Table 3
Capsize probability or risk in three coastal sectors of Kuwait in January to June based on Rayleigh-distributed wave heights and log-normally distributed annual maximum significant wave heights

| Vessel length (m) | Cap-size | Risk % | January | Cap-size | Risk % | February | Cap-size | Risk % | March | Cap-size | Risk % | April | Cap-size | Risk % | May | Cap-size | Risk % | June |
|---|---|---|---|---|---|---|---|---|---|---|---|---|---|---|---|---|---|---|
| | Sector A | Sector B | Sector C | Sector A | Sector B | Sector C | Sector A | Sector B | Sector C | Sector A | Sector B | Sector C | Sector A | Sector B | Sector C | Sector A | Sector B | Sector C |
| 3 | 0.8294 | 0.6806 | 10.7723 | 0.6501 | 0.6852 | 13.5507 | 1.7513 | 1.1588 | 20.6249 | 1.7513 | 1.1588 | 20.6249 | 0.2977 | 0.6803 | 7.8225 | 0.5806 | 0.8909 | 12.8137 |
| 4 | 0.1771 | 0.1172 | 3.7318 | 0.1118 | 0.0933 | 5.8271 | 0.3604 | 0.1947 | 8.9052 | 0.3604 | 0.1947 | 8.9052 | 0.035 | 0.1086 | 1.9492 | 0.1115 | 0.1761 | 5.6223 |
| 5 | 0.0424 | 0.0224 | 1.2743 | 0.022 | 0.0141 | 2.5829 | 0.081 | 0.0351 | 3.7423 | 0.081 | 0.0351 | 3.7423 | 0.0048 | 0.0196 | 0.4594 | 0.0249 | 0.0397 | 2.5656 |
| 6 | 0.0114 | 0.0048 | 0.445 | 0.0049 | 0.0024 | 1.1855 | 0.0198 | 0.0068 | 1.5664 | 0.0198 | 0.0068 | 1.5664 | 0.0007 | 0.004 | 0.1068 | 0.0063 | 0.01 | 1.2183 |
| 7 | 0.0034 | 0.0012 | 0.1607 | 0.0012 | 0.0004 | 0.5655 | 0.0053 | 0.0015 | 0.6641 | 0.0053 | 0.0015 | 0.6641 | 0.0001 | 0.0009 | 0.0252 | 0.0018 | 0.0028 | 0.6029 |
| 8 | 0.0011 | 0.0003 | 0.0601 | 0.0003 | 0.0001 | 0.2793 | 0.0015 | 0.0003 | 0.2864 | 0.0015 | 0.0003 | 0.2864 | 0 | 0.0002 | 0.0061 | 0.0005 | 0.0008 | 0.3094 |
| 9 | 0.0004 | 0.0001 | 0.0232 | 0.0001 | 0 | 0.1424 | 0.0005 | 0.0001 | 0.126 | 0.0005 | 0.0001 | 0.126 | 0 | 0.0001 | 0.0015 | 0.0002 | 0.0003 | 0.164 |
| 10 | 0.0001 | 0 | 0.0093 | 0 | 0 | 0.0747 | 0.0001 | 0 | 0.0565 | 0.0001 | 0 | 0.0565 | 0 | 0 | 0.0004 | 0.0001 | 0.0001 | 0.0894 |
| 11 | 0.0001 | 0 | 0.0038 | 0 | 0 | 0.0403 | 0.0001 | 0 | 0.026 | 0.0001 | 0 | 0.026 | 0 | 0 | 0.0001 | 0 | 0 | 0.0502 |
| 12 | 0 | 0 | 0.0016 | 0 | 0 | 0.0223 | 0 | 0 | 0.0122 | 0 | 0 | 0.0122 | 0 | 0 | 0 | 0 | 0 | 0.0288 |
| 13 | 0 | 0 | 0.0007 | 0 | 0 | 0.0126 | 0 | 0 | 0.0058 | 0 | 0 | 0.0058 | 0 | 0 | 0 | 0 | 0 | 0.0169 |
| 14 | 0 | 0 | 0.0003 | 0 | 0 | 0.0073 | 0 | 0 | 0.0028 | 0 | 0 | 0.0028 | 0 | 0 | 0 | 0 | 0 | 0.0101 |
| 15 | 0 | 0 | 0.0001 | 0 | 0 | 0.0043 | 0 | 0 | 0.0014 | 0 | 0 | 0.0014 | 0 | 0 | 0 | 0 | 0 | 0.0062 |
| 16 | 0 | 0 | 0.0001 | 0 | 0 | 0.0026 | 0 | 0 | 0.0007 | 0 | 0 | 0.0007 | 0 | 0 | 0 | 0 | 0 | 0.0038 |
| 17 | 0 | 0 | 0 | 0 | 0 | 0.0016 | 0 | 0 | 0.0004 | 0 | 0 | 0.0004 | 0 | 0 | 0 | 0 | 0 | 0.0024 |
| 18 | 0 | 0 | 0 | 0 | 0 | 0.001 | 0 | 0 | 0.0002 | 0 | 0 | 0.0002 | 0 | 0 | 0 | 0 | 0 | 0.0015 |
| 19 | 0 | 0 | 0 | 0 | 0 | 0.0006 | 0 | 0 | 0.0001 | 0 | 0 | 0.0001 | 0 | 0 | 0 | 0 | 0 | 0.001 |
| 20 | 0 | 0 | 0 | 0 | 0 | 0.0004 | 0 | 0 | 0.0001 | 0 | 0 | 0.0001 | 0 | 0 | 0 | 0 | 0 | 0.0006 |
| 21 | 0 | 0 | 0 | 0 | 0 | 0.0002 | 0 | 0 | 0 | 0 | 0 | 0 | 0 | 0 | 0 | 0 | 0 | 0.0004 |
| 22 | 0 | 0 | 0 | 0 | 0 | 0.0002 | 0 | 0 | 0 | 0 | 0 | 0 | 0 | 0 | 0 | 0 | 0 | 0.0003 |
| 23 | 0 | 0 | 0 | 0 | 0 | 0.0001 | 0 | 0 | 0 | 0 | 0 | 0 | 0 | 0 | 0 | 0 | 0 | 0.0002 |
| 24 | 0 | 0 | 0 | 0 | 0 | 0.0001 | 0 | 0 | 0 | 0 | 0 | 0 | 0 | 0 | 0 | 0 | 0 | 0.0001 |
| 25 | 0 | 0 | 0 | 0 | 0 | 0 | 0 | 0 | 0 | 0 | 0 | 0 | 0 | 0 | 0 | 0 | 0 | 0.0001 |

Table 4
Capsize probability or risk in three coastal sectors of Kuwait in July to December based on Rayleigh-distributed wave heights and log-normally distributed annual maximum significant wave heights

| Vessel length (m) | Cap-size | Risk % | July | Cap-size | Risk % | August | Cap-size | Risk % | September | Cap-size | Risk % | October | Cap-size | Risk % | November | Cap-size | Risk % | December |
|---|---|---|---|---|---|---|---|---|---|---|---|---|---|---|---|---|---|---|
| | Sector A | Sector B | Sector C | Sector A | Sector B | Sector C | Sector A | Sector B | Sector C | Sector A | Sector B | Sector C | Sector A | Sector B | Sector C | Sector A | Sector B | Sector C |
| 3 | 1.1061 | 1.1061 | 16.2642 | 0.4537 | 0.2978 | 11.6505 | 0.0055 | 0.0013 | 2.2347 | 0.0278 | 0.0271 | 3.6166 | 0.4392 | 0.5505 | 13.2158 | 0.0669 | 0.0551 | 6.2568 |
| 4 | 0.2762 | 0.2762 | 8.0495 | 0.0769 | 0.0368 | 5.52 | 0.0001 | 0 | 0.3183 | 0.0017 | 0.0015 | 0.8389 | 0.0623 | 0.0719 | 4.9886 | 0.0043 | 0.0021 | 1.2969 |
| 5 | 0.0789 | 0.0789 | 4.1382 | 0.0152 | 0.0053 | 2.7662 | 0 | 0 | 0.0439 | 0.0001 | 0.0001 | 0.2027 | 0.0102 | 0.0105 | 1.8859 | 0.0003 | 0.0001 | 0.246 |
| 6 | 0.0251 | 0.0251 | 2.2068 | 0.0034 | 0.0009 | 1.4545 | 0 | 0 | 0.0061 | 0 | 0 | 0.0517 | 0.0019 | 0.0017 | 0.7264 | 0 | 0 | 0.045 |
| 7 | 0.0088 | 0.0088 | 1.2209 | 0.0009 | 0.0002 | 0.7996 | 0 | 0 | 0.0009 | 0 | 0 | 0.014 | 0.0004 | 0.0003 | 0.2885 | 0 | 0 | 0.0083 |
| 8 | 0.0033 | 0.0033 | 0.6971 | 0.0002 | 0 | 0.4561 | 0 | 0 | 0.0001 | 0 | 0 | 0.004 | 0.0001 | 0.0001 | 0.1182 | 0 | 0 | 0.0015 |
| 9 | 0.0013 | 0.0013 | 0.4095 | 0.0001 | 0 | 0.2687 | 0 | 0 | 0 | 0 | 0 | 0.0012 | 0 | 0 | 0.05 | 0 | 0 | 0.0003 |
| 10 | 0.0006 | 0.0006 | 0.2464 | 0 | 0 | 0.1626 | 0 | 0 | 0 | 0 | 0 | 0.0004 | 0 | 0 | 0.0217 | 0 | 0 | 0.0001 |
| 11 | 0.0002 | 0.0002 | 0.1519 | 0 | 0 | 0.1009 | 0 | 0 | 0 | 0 | 0 | 0.0001 | 0 | 0 | 0.0097 | 0 | 0 | 0 |
| 12 | 0.0001 | 0.0001 | 0.0955 | 0 | 0 | 0.064 | 0 | 0 | 0 | 0 | 0 | 0 | 0 | 0 | 0.0045 | 0 | 0 | 0 |
| 13 | 0.0001 | 0.0001 | 0.0612 | 0 | 0 | 0.0414 | 0 | 0 | 0 | 0 | 0 | 0 | 0 | 0 | 0.0021 | 0 | 0 | 0 |
| 14 | 0 | 0 | 0.0398 | 0 | 0 | 0.0272 | 0 | 0 | 0 | 0 | 0 | 0 | 0 | 0 | 0.001 | 0 | 0 | 0 |
| 15 | 0 | 0 | 0.0263 | 0 | 0 | 0.0182 | 0 | 0 | 0 | 0 | 0 | 0 | 0 | 0 | 0.0005 | 0 | 0 | 0 |
| 16 | 0 | 0 | 0.0176 | 0 | 0 | 0.0123 | 0 | 0 | 0 | 0 | 0 | 0 | 0 | 0 | 0.0003 | 0 | 0 | 0 |
| 17 | 0 | 0 | 0.0119 | 0 | 0 | 0.0084 | 0 | 0 | 0 | 0 | 0 | 0 | 0 | 0 | 0.0001 | 0 | 0 | 0 |
| 18 | 0 | 0 | 0.0081 | 0 | 0 | 0.0058 | 0 | 0 | 0 | 0 | 0 | 0 | 0 | 0 | 0.0001 | 0 | 0 | 0 |
| 19 | 0 | 0 | 0.0056 | 0 | 0 | 0.0041 | 0 | 0 | 0 | 0 | 0 | 0 | 0 | 0 | 0 | 0 | 0 | 0 |
| 20 | 0 | 0 | 0.0039 | 0 | 0 | 0.0028 | 0 | 0 | 0 | 0 | 0 | 0 | 0 | 0 | 0 | 0 | 0 | 0 |
| 21 | 0 | 0 | 0.0027 | 0 | 0 | 0.002 | 0 | 0 | 0 | 0 | 0 | 0 | 0 | 0 | 0 | 0 | 0 | 0 |
| 22 | 0 | 0 | 0.0019 | 0 | 0 | 0.0014 | 0 | 0 | 0 | 0 | 0 | 0 | 0 | 0 | 0 | 0 | 0 | 0 |
| 23 | 0 | 0 | 0.0014 | 0 | 0 | 0.001 | 0 | 0 | 0 | 0 | 0 | 0 | 0 | 0 | 0 | 0 | 0 | 0 |
| 24 | 0 | 0 | 0.001 | 0 | 0 | 0.0007 | 0 | 0 | 0 | 0 | 0 | 0 | 0 | 0 | 0 | 0 | 0 | 0 |
| 25 | 0 | 0 | 0.0007 | 0 | 0 | 0.0005 | 0 | 0 | 0 | 0 | 0 | 0 | 0 | 0 | 0 | 0 | 0 | 0 |

unavoidably rather small to really differentiate between the three distributions with a high level of confidence. On this basis, the present study has used the lognormal distribution for evaluating the total risk via Eq. (12) coupled with Fig. 4. The parameters characterizing the lognormal distribution for all 12 months are summarized in Table 2 and the capsize risks associated with vessels of sizes varying from 3 to 25 m within each territorial sector, A, B or C, are given in the monthly shown in Tables 3 and 4.

## 4. Summary and conclusions

Kuwait's territorial waters were described in terms of three sectors A, B and C. Sectors A and B represent two relatively sheltered areas characterized by short wind fetches and/or shallower water depths protected by an offshore island. In contrast, sector C represents an area where wind fetches and water depths are significantly larger. The same sector is also unsheltered against winds, particularly from the South–East directions. Based on the assumption that the extreme or adverse wave conditions result from peak wind patterns with larger energy and coming from the South–East and North–West quadrants, these wind patterns and their times of occurrences were determined and then employed in the spectral wind-wave prediction model (Sulisz et al., 2000) to forecast the peak wave heights and corresponding wave periods, expressed in terms of monthly significant values, covering the eight-year period from 1993 to 2000. Laboratory experiments as in (Al-Salem, 2004) performed on models with a model length scale of 19, and representing a fairly wide range of dimensionless ratios of length/beam, beam/draft and depth/draft were then used as a basis for developing the threshold wave heights that can cause capsizing of prototype vessels of sizes from 3 to 25 m. This approach has subsequently allowed estimation of capsize risks associated with a vessel of given length in sectors A, B and C, assuming that the dimensionless ratios tested represent all or at least most vessel types registered in Kuwait. For the analysis, modeling and computation of capsize risks, the extremal lognormal distribution for peak significant wave heights was coupled with the Rayleigh distribution describing the relative occurrence of wave heights in a given sea state. This process has led to the estimates of monthly capsize risks associated with vessels of varying lengths in sectors A, B and C, as summarized in Tables 3 and 4. It is seen from these tables that sector C exposed to longer wind fetches with deeper water depths and thus, to more severe wave conditions is the critical region. The capsize risk associated with relatively small vessels, particularly those with lengths less than 7–8 m are noticeably high. In contrast, sectors A and B represent relatively safe regions for most vessels, particularly those with lengths longer than 4–5 m.

## References

Al-Salem, K., Al-Nassar, W.,Tayfun, A., 2004. Risk analysis of small vessels kuwait's marine environment. Kuwait Institute for Scientific Research, Report No. KISR 7358, Kuwait.

Sulisz, W., Al-Salem, K., Paplinska, B., Shuhaibar, B.B., Al-Amer, N., 2000. Prediction of wind waves for Kuwaits territorial waters. Kuwait Institute for Scientific Research, Report No. KISR5787, Kuwait.